NASA TECHNICAL MEMORANDUM

NASA TM X-52988

NASA TM X-52988

VELOCITY AND TEMPERATURE PROFILES IN NEAR-CRITICAL NITROGEN

by Robert J. Simoneau, James C. Williams III,
and Robert W. Graham
Lewis Research Center
Cleveland, Ohio

TECHNICAL PAPER proposed for presentation at
National Heat Transfer Conference sponsored by
the American Society of Mechanical Engineers
Tulsa, Oklahoma, August 15-18, 1971

VELOCITY AND TEMPERATURE PROFILES IN NEAR-CRITICAL NITROGEN

by Robert J. Simoneau
National Aeronautics and Space Administration
Lewis Research Center
Cleveland, Ohio

James C. Williams III
North Carolina State University
Raleigh, North Carolina

and Robert W. Graham
National Aeronautics and Space Administration
Lewis Research Center
Cleveland, Ohio

ABSTRACT

Boundary layer velocity and temperature profiles were measured in nitrogen near its thermodynamic critical point flowing turbulently upward over a heated flat plate with constant surface heat flux. The measurements were made with a combination thermocouple and pitot-static probe.

Data were taken with the fluid in the boundary layer spanning the critical temperature and also at the same operating conditions except with the boundary layer at temperatures away from the critical temperature. These results showed that the near-critical velocity profiles were quite different, exhibiting a maximum between the wall and free stream. The near-critical profile had a much larger Grashof number suggesting that a strong body force effect was present. The data are examined in terms of the velocity and temperature profile response to variations in the system parameters. Proximity to the critical point appears to exaggerate body forces even at quite high Reynolds numbers.

NOTATION

D tube diameter, mm

g acceleration of gravity, cm/sec^2

Gr_x Grashof number, $\rho_\infty(\rho_\infty - \rho_w)x^3g/\eta_\infty^2$

h heat transfer coefficient, $W/cm^2\ ^oK$

L tube length, mm

P pressure, atm

q heat flux, W/cm^2

Re_x Reynolds number, $\rho_\infty u_\infty x/\eta_\infty$

T temperature, ^oK

u velocity, m/sec

x distance from leading edge of plate, cm

y normal distance from the plate, mm

η dynamic viscosity, gm/cm-sec

ρ density, gm/cm^3

Subscripts

b fluid bulk conditions

c critical point conditions

w wall conditions

x conditions at axial position x along the plate

∞ free stream conditions

Superscript

* transposed critical point conditions - temperature as a function of pressure at which the constant pressure specific heat curve maximizes

INTRODUCTION

Because of the strong, nonlinear thermal property variations of fluids near the thermodynamic critical point, heat transfer, and fluid flow of near-critical fluids are challenging research and design problems. In recent years the necessity of operating near the critical point has complicated the design analyses of hydrogen rocket engines, high pressure steam generating systems and cryomagnets. In the future, the possible use of supercritical methane as an aviation fuel may present a similar problem.

The field has been actively researched for about 25 years. This research has been comprehensively surveyed in recent articles by Hendricks et al. (1), Hall et al. (2), and Petukov (3). It is apparent from these surveys that there exists a lack of data of sufficient detail to make an accurate description of the velocity and temperature fields, especially in forced convection. This in turn has hampered the selection of a realistic model for analysis. The literature does not lack suggested analyses. What is lacking are the velocity and temperature profile data needed to definitively test a given flow model.

Only two experiments have been performed in which profile measurements have been made during heat transfer

to a near-critical fluid. Wood (4, 5) and Wilson (6) both made velocity and temperature surveys near the exit of a smooth tube with a constant heat flux boundary condition. Wood (4, 5) flowed carbon dioxide vertically upward in a 22.9 mm diameter tube. He made measurements at L/D = 30.7, and could survey to within 0.25 mm of the wall. He observed that under conditions of $T_b < T^* < T_w$ the temperature profiles flattened considerably and heat transfer coefficients rose sharply as the bulk fluid approached the critical temperature. He also observed that the velocity profile achieved its maximum value between the wall and centerline, yielding a characteristic M-shape. His experiment was hampered somewhat by the fact that the velocity and temperature profile measurements were made separately, requiring matching of two runs. At present no analyses of Wood's data have been published. Wilson (6) flowed hydrogen, also vertically upward, at L/D = 128.5 in a 35.0 mm diameter tube. Wilson could not make measurements as close to the wall as Wood; however, he employed a combined thermocouple, hot wire, and pitot probe and took continuous data. Wilson's results confirmed the presence of the M-shaped profile and exhibited a great deal of noise in the profile traces. Wilson's results also showed a strong spike in the wall temperature distribution axially along the tube (see also (1)). Wilson correlated his data using a pseudo-boiling model.

The potential of using the hot wire in the near-critical region has also been examined by Bourke et al. (7) in adiabatic tests with CO_2. Despite our lack of knowledge of the heat transfer processes in this region the hot wire shows real promise for meaningful measurements.

In addition to these velocity and temperature survey experiments, Sabersky and Hauptmann (8) published some outstanding color photographs of a near-critical carbon dioxide boundary layer on a horizontal flat plate. These pictures coupled with the data, including hot wire signals measured at 0.25 mm above the plate, gave some insight into the nature of the flow. They concluded that the flow could be treated as single phase turbulent flow, possibly requiring modifications for enhanced turbulent fluctuations.

Recently several investigators (9-14) have directed their attention to the phenomenon of the large increase or "spike" that occurs in the wall temperature under constant surface heat flux conditions in near-critical fluids flowing in smooth tubes. It was found that the "spike" could be attenuated mechanically (e.g., swirl devices) (10, 13, 14) or by the presence of a strong body force effect (9-13). While the wall temperature spike is not studied in the present experiment, strong body force effects did occur and the above investigations are related accordingly. In these tube experiments (9-13) the body force effect was demonstrated by flowing both upward and downward. It was determined that body forces would influence the wall temperature if the Grashof number divided by the square of the Reynolds number were greater than 10^{-2}. The numeric value will of course depend on the definition of Reynolds and Grashof numbers; it is the parametric grouping that is of interest.

Many analyses and flow models have been directed toward near-critical heat transfer. The present results should be of particular interest in testing the various modifications of mixing length theory proposed over the years (15-21). Of special interest is the work of Hsu and Smith (17) because it included the body force effect and predicted the Grashof-Reynolds relationship mentioned above.

The present study was undertaken to obtain velocity and temperature boundary layer profiles in a geometry which was as simple as possible. This was done by flowing near-critical nitrogen vertically upward over a flat plate having a constant heat flux at the surface. The effort here was to avoid some of the complex phenomena that occur in tubes - particularly the wall temperature spike. Wilson (6), for instance, reported the wall temperature spike, whereas Wood (4, 5) did not. It was felt that the simpler geometry would be more amenable to analysis. Furthermore, the flat plate configuration allows more parametric control. For instance, the fluid free stream properties can be controlled independent of the surface heat flux, which is not the case in tubes. It should be emphasized that the tube data are very important and closer to reality. The present work intends to complement that of Wood (4, 5) and Wilson (6).

The range of operating conditions obtained are indicated on Fig. 1, the density curve for near-critical nitrogen at $P/P_c = 1.10$. The thermal properties were obtained from a computer program of Pew et al. (22), which employed the equation of state of Strobridge (23) and the viscosity correlation of Brebach and Thodos (24). Of all the strongly varying properties associated with the critical point, it is the density which appears to play the most important role. In the present experiment data were acquired at operating conditions such that: (1) both the wall and free stream were below the critical temperature, (2) both the wall and free stream were above the critical temperature, and finally, (3) the wall was above and the free stream was below the critical temperature. The data presented herein are bounded by the following ranges of the parameters. Of course, not all combinations were covered.

$$P_\infty/P_c \approx 1.10$$

$$0.70 < T_\infty/T_c < 0.99$$

$$0.80 < T_w/T_c < 1.75$$

$$0 < q < 15\ W/cm^2$$

$$7.0\times10^5 < Re_x < 17.5\times10^5$$

$$P_c = 33.5\ atm,\ T_c = 126.2^o\ K,\ \rho_c = 0.311\ gm/cm^3$$

The data will be presented in a manner as to illustrate the influence of parameters such as: free stream temperature, surface heat flux, Reynolds number and Grashof number on the boundary layer profiles.

EXPERIMENTAL APPARATUS

The experiment can best be described by thinking of it in terms of a conventional wind tunnel, except here the fluid is near-critical nitrogen flowing at about 1 meter per second. The test apparatus is illustrated schematically in

Fig. 2. It was a once-through or blow-down type system. Liquid nitrogen was transferred from a low pressure supply to the 0.4 m^3 high pressure dewar. The fluid temperature was controlled by bubbling nitrogen gas through the dewar. Nitrogen gas, at the desired pressure, was applied to the top of the fluid to force the fluid through the system. System pressure and flow rate were maintained by the use of throttling valves. The system was heavily insulated and was precooled from an auxiliary supply. The once-through system avoided the problem of pump oscillations, but not the system oscillations characteristic of near-critical fluids (1).

The test section was of rectangular cross-section of about 6 to 5 aspect ratio. It contained two 2.5 cm wide by 15 cm long nichrome plates back to back. The first centimeter was a copper electrode and was unheated. The primary surface was instrumented longitudinally with 11 chromel-constantan thermocouples electrically isolated from the heater. The opposite surface served as a guard heater and was also instrumented. Heat was generated by the dissipation of direct-current power. Figure 3 is a photograph of the heater plate assembly.

The boundary layer surveys were made with a combination pitot-static and thermocouple probe which was traversed through the boundary layer toward the primary heater surface. The distance from the primary heater surface to the opposite wall was about 2.4 cm, which was approximately 10 times the boundary layer thickness computed from a 1/7th power profile. On the back side the distance to the wall was 0.72 cm, about 3 times the computed boundary layer thickness. The temperature portion of the probe was an exposed ball, chromel-constantan thermocouple encased in a sheath with an overall diameter of 0.20 mm. The dynamic pressure part of the probe was a two leg pitot-static probe of rectangular cross-section at the tip and had an overall tip height of 0.20 mm. Pictures of the actual probe are shown in Fig. 4. The total pressure leg had a 0.075×0.70 mm opening at the tip. The static port was a 0.25 mm diameter hole located six thicknesses from the tip to avoid separation. Measurements could be made to within 0.10 mm of the wall. All of the surveys reported herein were made 13.1 cm from the leading edge of the plate.

An important feature of this design was making both legs identical. This was done in order to match the response lags in the lines, reducing the noise, and also to assure the same density gradient in each leg to avoid static head errors. The probe noise was assessed to be due to very small static pressure perturbations. This is discussed in detail in (25). Wood (4, 5) and Wilson (6) both observed probe noise. Wilson's level of noise was about the same order as in the present experiment.

Flow rates were measured with venturi flow meters. All system pressures were measured with strain gage transducers, except at the probing station where the system static pressure was measured with a high precision transducer accurate to ±0.05%. The dynamic head was measured with a variable reluctance type transducer. System temperatures were measured with platinum resistance thermometers. The heater plate thermocouples were standard chromel-constantan. All signals, including test section voltage and current, were sensed with a precision digital voltmeter and recorded on a digital data acquisition system. All measurements were checked by some kind of redundant instrument. The accuracies of the major parameters based on percent of the average value measured are presented in Table I.

Table I. - Accuracy of Major Parameters Based on the Average Value Measured

Free stream temperature	±0.2%	±0.2° K
Free stream pressure	±0.1%	±0.04 atm
Free stream density	±1.0%	±0.006 gm/cm^3
Free stream velocity	±1.5%	±0.02 m/sec
Mass flow rate	±1.3%	±0.008 kg/sec
Heat flux	±1.0%	±0.1 W/cm^2
Wall temperature	±1.0%	±2° K
Probe temperature	±0.5%	±0.5° K
Dynamic pressure	±2.0%	±0.001 psi

The manner in which the data were taken has a bearing on the results, particularly the number of points which could be acquired during a probe traverse. The system was brought up to nominal operating conditions and allowed to stabilize on some near-nominal operating condition. At this point a traverse of the probe from the free stream to the plate was begun. The traverse was made by moving the probe in about 15 discrete steps, stopping at each step to acquire data. Because of the probe noise mentioned earlier, at each step the signals were electronically integrated for about 3 seconds. Then the integrated signals and all system parameters were recorded and the probe was moved to the next position. Because of the blow down configuration, this procedure limited the number of points per traverse to about 15.

The test apparatus, instruments, data accuracy, operating procedure, and probe noise are discussed in detail in (25).

RESULTS

Prior to the actual data runs adiabatic profiles in both gas and near-critical nitrogen were obtained upstream of the heater plate. These were integrated for mass flow rate and the results compared very favorably with the values from both flow meters (fig. 2). These measurements also indicated that the profile approaching the plate was flat for a distance of 10 mm above the plate. Profiles measured over the plate in both adiabatic and heated nitrogen gas exhibited power law behavior. The adiabatic near-critical profiles over the plate also exhibited power law behavior. This is all documented in (25). This preliminary information was used to establish confidence in the measurements.

In order to obtain an overall view of the results of the present study, it is of interest to examine the velocity and temperature profiles of a near-critical fluid in comparison to the same fluid under the same conditions except at free stream temperatures away from the critical temperature. These data are presented in Figs. 5 and 6. The thermodynamic ranges covered by these three runs are

those denoted on the density curve, Fig. 1. In Fig. 5 the low density, or "gas," and the high density, or "liquid" velocity profiles fall virtually on top of each other and are in the 1/6th to 1/7th power range. The near-critical profile on the other hand is quite unusual in appearance, exhibiting a maximum near the wall. This is certainly consistent with the M-shaped profiles measured by Wood (4, 5) and Wilson (6) in pipes. The Grashof number associated with the near-critical profile is substantially greater than the others. This suggests that the unusual velocity profile is the result of the large density gradient across the boundary layer producing a strong body force effect, even though the Reynolds number is close to one million. This is consistent with the results of the recent upflow and downflow tube tests (9-13). The near-critical temperature profile is considerably flatter than those for the same fluid away from the critical point.

After illustrating the unusual nature of near-critical flow fields, it then becomes of interest to examine the influence of various system parameters on near-critical velocity and temperature profiles.

In Figs. 7 and 8 the influence of free stream temperature on near-critical velocity and temperature profiles is illustrated. At the lowest temperature, 89° K (T_c = 126.2° K), the velocity profile appears quite conventional in shape. An increase of 10° K toward the critical temperature yields a profile that is virtually flat over the majority of the boundary layer. Several of these "flat" velocity profiles occurred in the course of the experiment and they will be commented on later. A continued increase of free stream temperature 10° K toward the critical temperature yields a velocity profile with a maximum near the wall, similar to that displayed in Fig. 5. Further increases in free stream temperature toward the critical temperature produce velocity profiles which apparently peak closer and closer to the wall. The peak cannot be recorded in these cases because of the limitation on probe travel. Corresponding to these velocity profile changes is a change in Grashof number of a factor of 15.

The temperature profiles, Fig. 8, become increasingly flat as the free stream temperature approaches the critical temperature. This is consistent with Wood's results (4). On the other hand the trend in heat transfer coefficients is not consistent with Wood's. He showed a strong increase in heat transfer coefficient as the bulk fluid approached the critical temperature. The present results appear to indicate a decrease. The difference appears to lie in the fact that the present results were obtained at constant Reynolds number, while Wood's results were at constant velocity (4). Observe that at constant Reynolds number the velocity changes a factor of 2 in the present experiment. This suggests that the question of whether heat transfer coefficient increases or decreases near the critical point is somewhat a function of the path along which it is examined.

After reviewing the influence of free stream temperature on the velocity and temperature profiles the question arises as to whether or not the profile behavior is strictly a function of the free stream conditions. This can be examined by holding all the free stream conditions - particularly temperature - constant while varying surface heat flux. The results of this investigation are shown in Fig. 9. It can be seen from Fig. 9 that varying heat flux and holding free stream conditions constant produces the same velocity profile behavior as varying free stream temperature (cf., fig. 7).

Two facts are common to both sets of data. When the unusual velocity profiles occur, the wall temperature is above and the free stream temperature is below the critical temperature and the Grashof number has increased significantly. When the unusual velocity profiles occur the conditions are such that the sharp property changes associated with the critical point occur within the boundary layer. The condition of the wall-to-free stream temperature spanning the critical temperature can be achieved either by increasing the free stream temperature towards the critical point holding heat flux constant or by increasing heat flux holding free stream conditions constant.

The above tests were all run under a condition of constant free stream Reynolds number. Figure 10 shows the effect of varying Reynolds number holding free stream temperature and surface heat flux constant. This effectively varies the forces in the flow field mechanically as opposed to thermodynamically as in the above cases. Again the complete range of profile shapes can be produced. This result is particularly significant because it indicates that sufficiently high inertia forces can diminish the influence of the strong density change. Notice that the wall temperature in all cases in Fig. 10 is above the critical temperature, making the density gradient large and the Grashof number quite high. Still the Reynolds numbers are high enough in some of the cases to return the profiles to a somewhat normal shape.

The central theme then of these Fig. 7 to 10 is that the velocity profiles can be discussed in terms of conventional interactions of viscous, inertia, and body forces as expressed in standard nondimensional numbers, the Reynolds and Grashof numbers. The fact that the flow field responds in an expected manner to variations in conventional nondimensional parameters suggests that analyses based on turbulent mixing, such as suggested by Deissler (15), would be productive. The incorporation of a variable density in the manner of (16-20) would appear to be important. The data indicates that the inclusion of the body force term, as has been done by Hsu and Smith (17), is necessary, even at very high Reynolds numbers.

It has been pointed out that the parametric relationship Gr/Re^2 is considered significant in assessing the role of body force in near-critical heat transfer (9-11, 17). The determination of when body forces are significant requires a certain arbitrary element in the choice. In the tube experiments the demarcation was established as the point where there was no significant differences in heat transfer between upward and downward flow. For the moment, in the present experiment, the appearance of profiles which are "flat" to within 0.25 mm offer a possible hinge point. Five such profiles occurred in the experiment; three appear in Figs. 7, 9, and 10. They occur in a range:

$$1.6 < Gr_x/Re_x^2 < 3.0$$

The actual criterion should probably be lower, since when the profiles are "flat" body forces are already significant. However, since the "flat" profiles occur in a narrow range of Gr_x/Re_x^2, they probably can serve as a convenient and significant reference condition. The spread in Gr_x/Re_x^2 above is not strictly random scatter. There appears to be a heat flux influence; however, there is no clear trend. It may be, however, that Gr_x/Re_x^2 is an oversimplification.

While the evidence appears strong that body forces are significant in the present results, other forces, such as axial acceleration, could also be important. Tests performed in downward or horizontal flow could be definitive on this question and would be a logical extension of the present experiment.

In a few instances it was possible to obtain high speed (5000 frame/sec) movies of the near-critical boundary layer during a probe traverse. One set of these are shown along with the corresponding velocity profile data in Fig. 11. The view is across the plate; the flow is upward; and the probe is traversing right to left. Each picture is a single frame from a roll of film, which was taken with the probe stationary at the position indicated by the solid circles. The plate surface cannot be seen since the backlighting would not penetrate the boundary layer. The approximate position of the wall and the probe tip is marked with arrows in the photographs. Note that as the probe nears the wall it disappears into the boundary layer.

The photographs indicate a highly agitated boundary layer. They could be interpreted as a high level of turbulence. On the other hand, the photographs could be cited as similar to "film boiling." These photographic results are qualitative and open to multiple interpretations.

CONCLUSIONS

The main objective of this work was to make detailed velocity and temperature profile measurements near the thermodynamic critical point. The geometry was kept simple both for subsequent analysis and to avoid complex flow interactions, thus highlighting the influence of the strongly varying near-critical properties. A sufficiently wide range of parameters to illustrate the various flow patterns was examined. Typical data have been presented herein.

When compared to nitrogen in a state condition away the critical point but under the same operating conditions, the velocity profiles in near-critical nitrogen are quite unusual frequently exhibiting a maximum in the region between the wall and free stream.

Systematic investigation over a wide range of near-critical operating parameters reveals that velocity profiles over a vertical flat plate in the critical region exhibit a strong body force effect. It appears that the property variations, particularly density, are such as to make body forces significant even at very high Reynolds numbers. Body forces are significant where Gr_x/Re_x^2 is on the order of one.

The near-critical temperature profiles become increasingly flat as the free stream fluid approaches the critical temperature.

The fact that the velocity profiles respond in an expected manner when traditional parameters, such Reynolds and Grashof number, are varied suggests that the flow field can be characterized by turbulent flow models. The turbulent flow models in the literature wh...d include density gradient and body force effects are suggested as the first avenue of analysis of the present data.

REFERENCES

1 Hendricks, R. C., Simoneau, R. J., and Smith, R. V., "Survey of Heat Transfer to Near Critical Fluids," Advances in Cryogenic Engineering, Vol. 15, K. D. Timmerhaus, ed., Plenum Press, New York, 1970, pp. 197-237.

2 Hall, W. B., Jackson, J. D., and Watson, A., "A Review of Forced Convection Heat Transfer to Fluids at Supercritical Pressures," Symposium on Heat Transfer and Fluid Dynamics of Near Critical Fluids, Proceedings of the Institution of Mechanical Engineers, Vol. 182, Part 3I, 1968, pp. 10-22.

3 Petukhov, B. S., "Heat Transfer in a Single-Phase Medium Under Supercritical Conditions," High Temperature, Vol. 6, No. 4, July-Aug. 1968, pp. 696-709.

4 Wood, R. D., "Heat Transfer in the Critical Region: Experimental Investigation of Radial Temperature and Velocity Profiles," Ph.D. Thesis, 1968, Northwestern University, Evanston, Ill.

5 Wood, R. D. and Smith, J. M., "Heat Transfer in the Critical Region - Temperature and Velocity Profiles in Turbulent Flow," AIChE Journal, Vol. 10, No. 2, Mar. 1964, pp. 180-186.

6 Wilson, M., "Flow and Thermal Characteristics of Hydrogen Near Its Critical Point in a Heated Cylindrical Tube," Ph.D. Thesis, 1969, University of New Mexico, Albuquerque, N. M. (Los Alamos Scientific Lab. Report LA-4172).

7 Bourke, P. J., Pulling, D. J., Gill, L. E., and Denton, W. H., "Measurement of Turbulent Velocity, and Temperature Fluctuations in the Supercritical Region," Symposium on Heat Transfer and Fluid Dynamics of Near Critical Fluids, Proceedings of the Institution of Mechanical Engineers, Vol. 182, Part 3I, 1968, pp. 58-67.

8 Sabersky, R. H and Hauptmann, E. G., "Forced Convection Heat Transfer to Supercritical Pressure Carbon Dioxide," International Journal of Heat and Mass Transfer, Vol. 10, No. 11, Nov. 1967, pp. 1499-1508.

9 Shiralkar, B. S and Griffith, P., "Deterioration in Heat Transfer to Fluids at Supercritical Pressure and High Heat Fluxes," Journal of Heat Transfer, Vol. 91, No. 1, Feb. 1969, pp. 27-36.

10 Shiralkar, B. and Griffith, P., The Effect of Swirl, Inlet Conditions, Flow Direction, and Tube Diameter on the Heat Transfer to Fluids at Supercritical Pressure," Journal of Heat Transfer, Vol. 92, No. 3, Aug. 1970, pp. 465-474.

11 Jackson, J. D. and Evans-Lutterodt, K., "Impairment of Turbulent Forced Convection Heat Transfer to Supercritical Pressure CO_2 Caused by Buoyancy Forces," Research Rep. N.E.2, 1968, University of Manchester, Manchester, England.

12 Bourke, P. J., Pulling, D. J., Gill, L. E., and Denton, W. H., "Forced Convective Heat Transfer to Turbulent CO_2 in the Supercritical Region," International Journal of Heat and Mass Transfer, Vol. 13, No. 8, Aug. 1970, pp. 1339-1348.

13 Kamenetsky, B. and Shitsman, M., "Experimental Investigation of Turbulent Heat Transfer to Supercritical Water in a Tube With Circumferentially Varying Heat Flux," Heat Transfer 1970, Proceedings of the Fourth International Heat Transfer Conference, 1970, Paper No. B.8.10.

14 Ackerman, J. W., "Pseudoboiling Heat Transfer to Supercritical Pressure Water in Smooth and Ribbed Tubes," Journal of Heat Transfer, Vol. 92, No. 3, Aug. 1970, pp. 490-498.

15 Deissler, R. G., "Heat Transfer and Fluid Friction for Fully Developed Turbulent Flow of Air and Supercritical Water with Variable Fluid Properties," ASME Transactions, Vol. 76, No. 1, Jan. 1954, pp. 73-85.

16 Goldmann, K., "Heat Transfer to Supercritical Water and other Fluids with Temperature Dependent Properties," Chemical Engineering Progress Symposium Series, Vol. 50, No. 11, 1954, pp. 105-113.

17 Hsu, Y. Y., and Smith, J. M., "The Effect of Density Variation on Heat Transfer in the Critical Region," Journal of Heat Transfer, Vol. 83, No. 2, May 1961, pp. 176-182.

18 Melik-Pashaev, N. I., "Calculation of Convective Heat Transfer at Supercritical Pressure," High Temperature, Vol. 4, No. 6, Nov.-Dec. 1966, pp. 789-798.

19 Tanaka, H., Nishiwaki, N., and Hirata, M., "Turbulent Heat Transfer to Supercritical Carbon Dioxide," JSME 1967 Semi-International Symposium, 1967, pp. 127-134.

20 Hall, W. B., Jackson, J. D., and Kahn, S. A., "An Investigation of Forced Convection Heat Transfer to Supercritical Pressure Carbon Dioxide," Proceedings of the Third International Heat Transfer Conference, Vol. 1, AIChE, New York, pp. 257-266, 1966.

21 Hall, W. B., and Jackson, J. D., "Laminarization of a Turbulent Pipe Flow by Buoyancy Forces," ASME Paper No. 69-HT-55, Aug. 1969.

22 Pew, K. A., Hendricks, R. C., and Simoneau, R. J., "NTWO - A Nitrogen Properties Package," Advances in Cryogenic Engineering, Vol. 16, K. D. Timmerhaus (ed.), Plenum Press, New York, 1971.

23 Strobridge, T. R., "The Thermodynamic Properties of Nitrogen from 64 to 300° K Between 0.1 and 200 Atmospheres," Tech. Note 129, 1962, National Bureau of Standards.

24 Brebach, W. J., and Thodos, G., "Viscosity-Reduced State Correlation for Diatomic Gases," Industrial and Engineering Chemistry, Vol. 50, No. 7, July 1958, pp. 1095-1100.

25 Simoneau, R. J., Velocity and Temperature Profiles in Near-Critical Nitrogen Flowing over a Heated Flat Plate. Ph.D. Thesis, 1970, North Carolina State University, Raleigh, N.C.

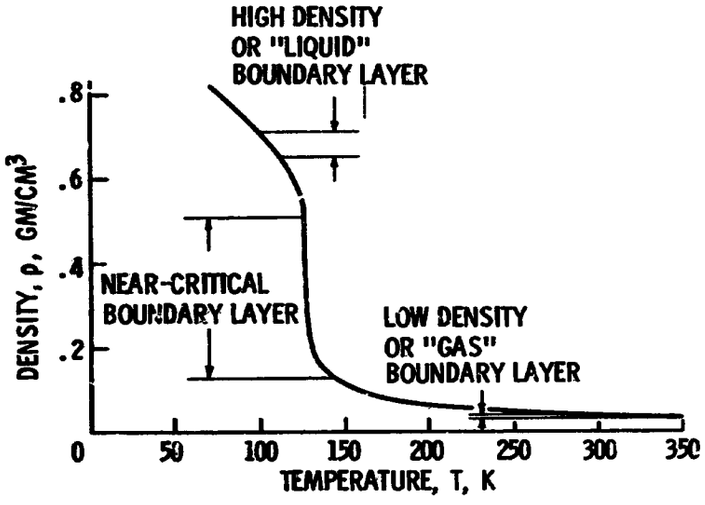

Figure 1. - Density of nitrogen as a function of temperature at $P/P_c = 1.10$ (refs. 22 and 23).

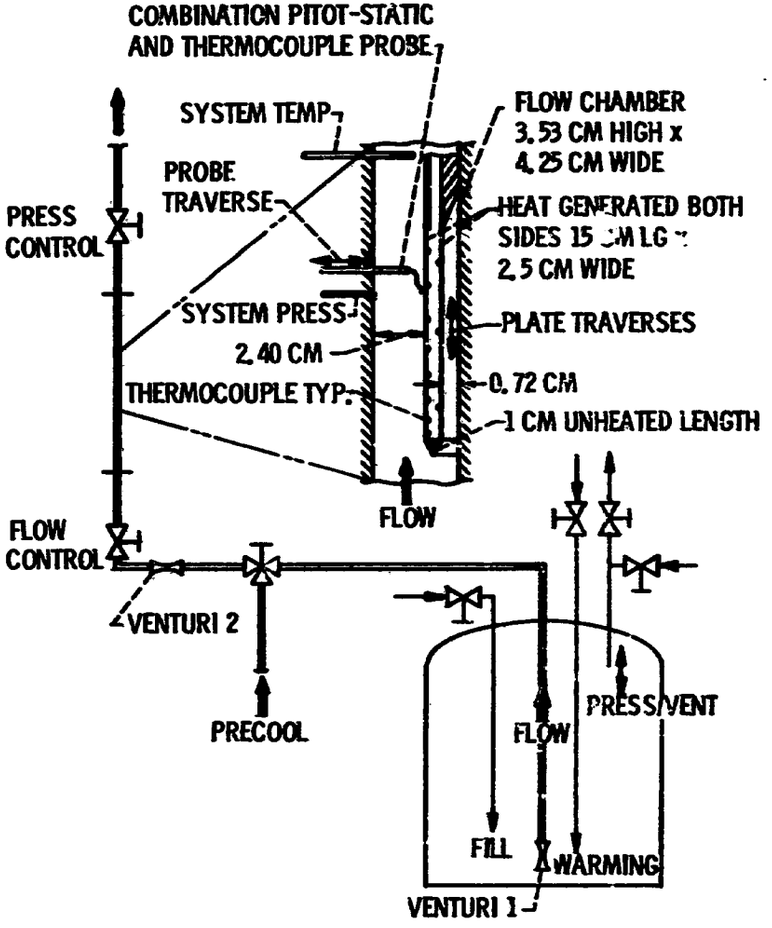

Figure 2. - Flow system and test section schematic.

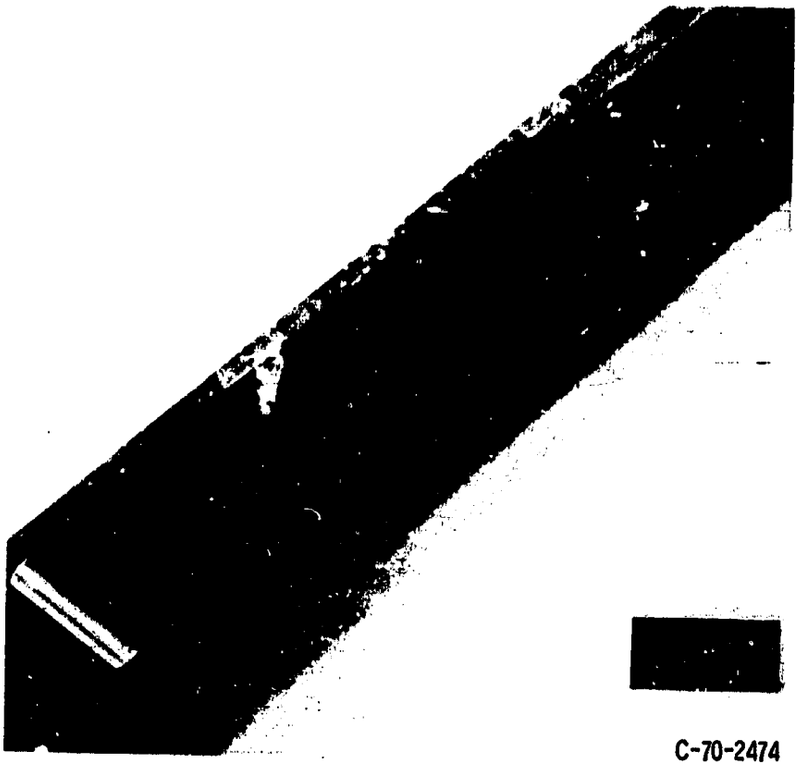

C-70-2474

Figure 3. - Heater plate assembly.

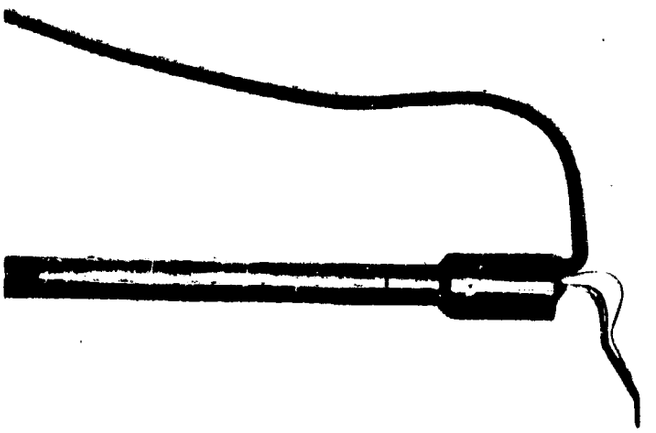

(a) Overall view (actual size).

(b) View at 45° angle from the tip (approx. 8 times actual size).

(c) View looking directly at the tip (approx. 21 times actual size).

Figure 4. - Actual photographs of combination pitot-static and thermocouple probe.

	RUN	FLUID STATE	u_∞, M/SEC	T_∞, K	T_w, K	q, WATTS/CM^2	RE_x, $\times 10^{-5}$	GR_x $\times 10^{-12}$
○	26	NEAR CRITICAL	0.511	124.4	143	3.06	9.48	3.30
□	8	LIQUID	0.833	99.2	110	3.07	9.03	0.144
△	39	GAS	2.61	272	341	3.14	9.04	.034

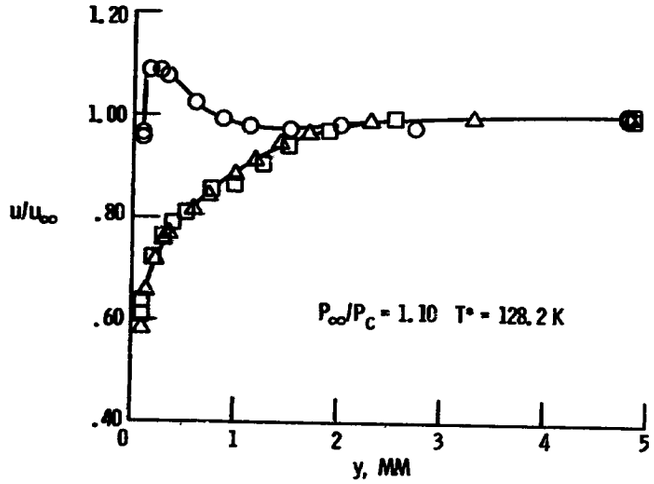

Figure 5. - Comparison of near-critical velocity profile to "gas" and "liquid" profiles under the same conditions.

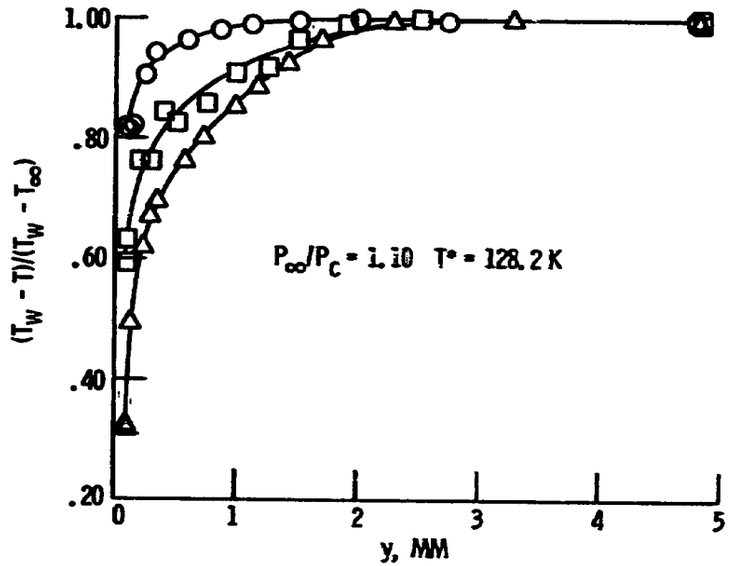

Figure 6. - Comparison of near-critical temperature profile to "gas" and "liquid" profiles under the same conditions.

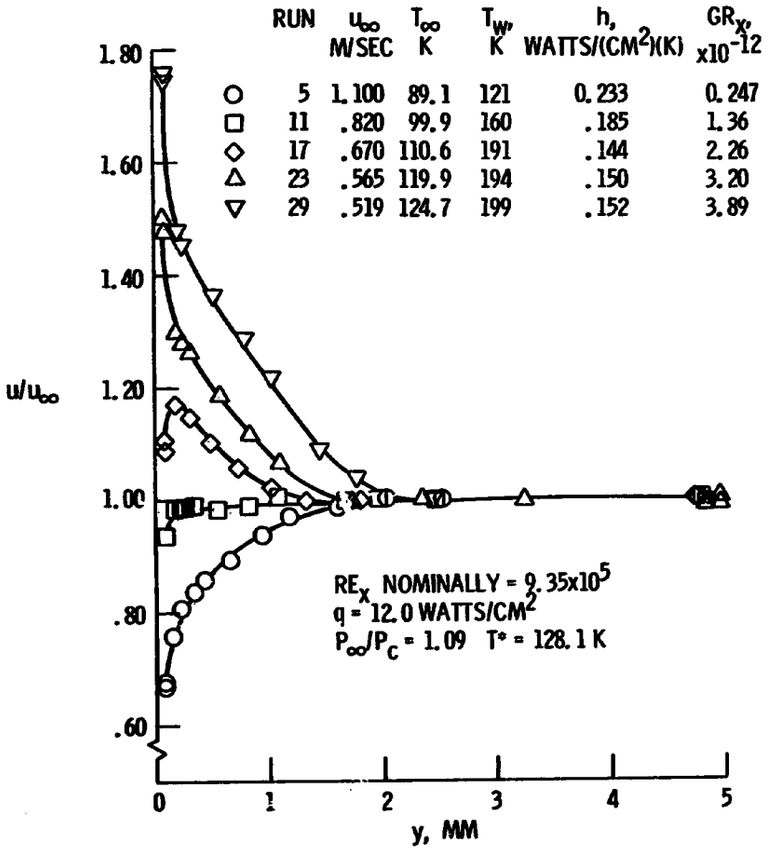

Figure 7. - Effect of free stream temperature on near-critical velocity profiles.

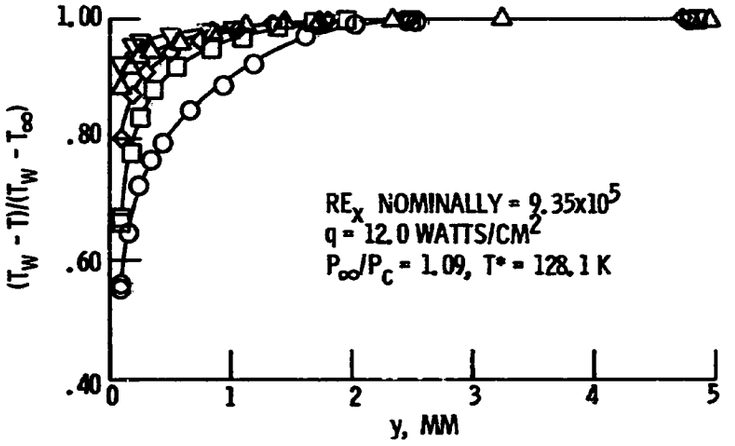

Figure 8. - Effect of free stream temperature on near-critical temperature profiles.

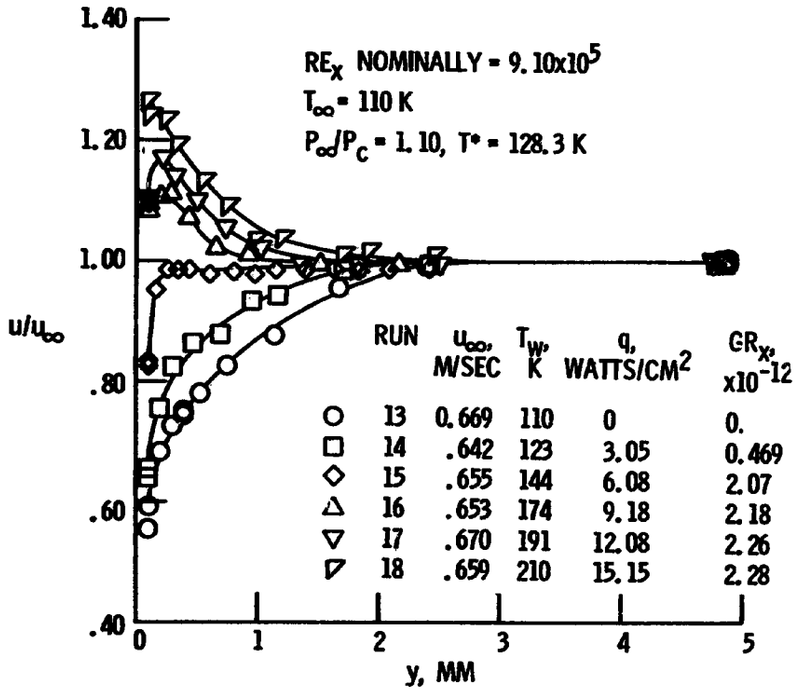

Figure 9. - Effect of heat flux on near-critical velocity profiles.

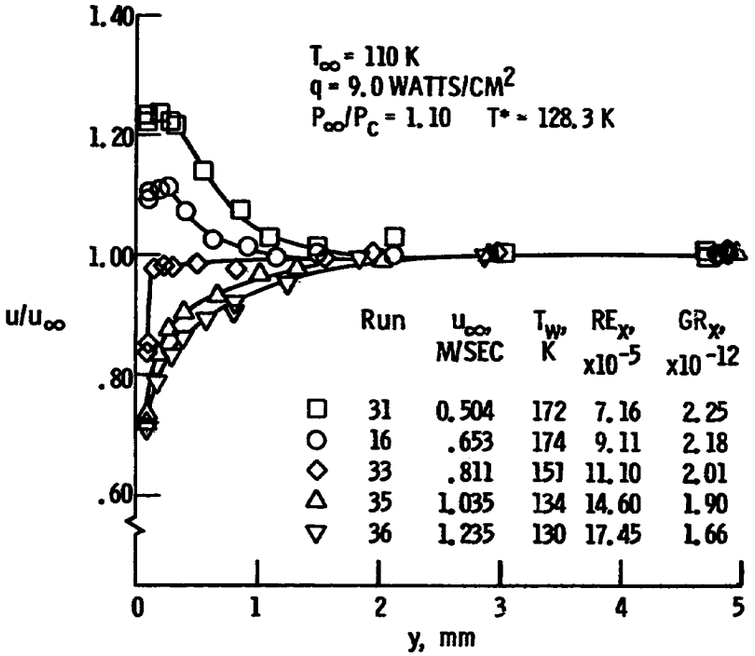

Figure 10. - Effect of Reynolds number on near-critical velocity profiles.

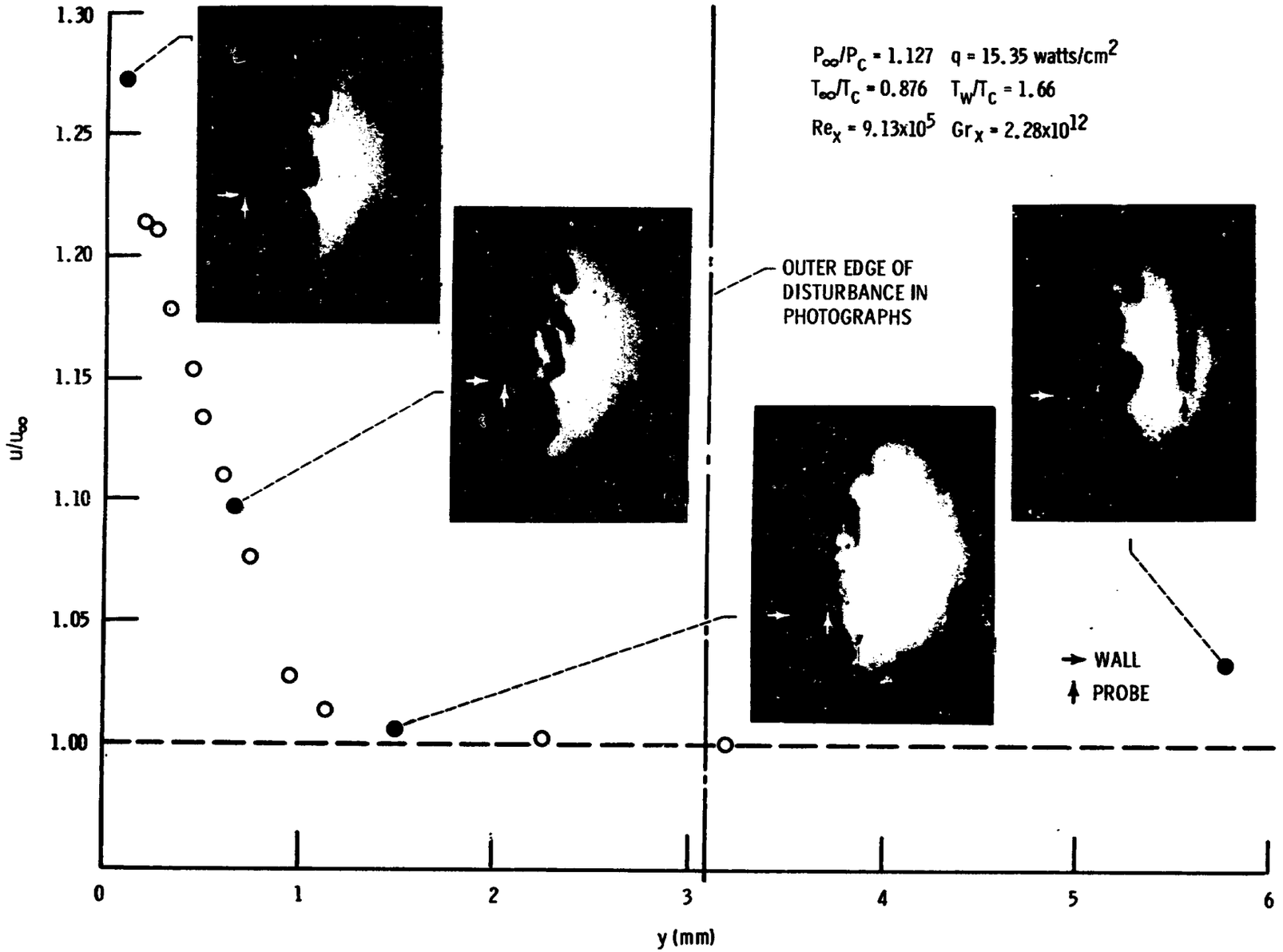

Figure 11. - Photographs of the near-critical boundary layer.